

Chapter 2

Formal description of transfer

The analysis of parasitics, as discussed in section 1.2.3, is of basic importance for wideband feedback design. Designers can analyze parasitic effects when they are adequately quantified.

Quantification of parasitics requires an unambiguous definition of transfer properties of devices. The basis of an adequate transfer description, including parasitic interactions, is a proper description of wideband *signals*. This is essential since signal flow is highly affected by the geometry of the print layout on the transport of signal to the devices.

This chapter provides these theoretical tools, and starts with a detailed description of complex signal flow (magnitude and phase) in a well-defined geometry. It summarizes the formal definitions of load impedances, sources, and transfer in arbitrary multi-port networks. All discussions are focused on *linear* descriptions.

Highlights of this chapter

In this chapter, a (micro)wave approach for describing signals and devices is followed. It relies on known concepts¹ of waves, reference planes and matrix parameters to describe devices as blackboxes. All these aspects are discussed in this chapter.

The highlights of this chapter, which have been explored in this study, are:

- A detailed overview of known definitions and relations on signal flow through reference planes. It is applicable to voltages and currents as well as to waves normalized to arbitrary (complex) reference impedances.
- A detailed overview of known matrix methods for describing one-port, two-port and multi-port networks, and for describing their properties and relations. The validity of the formulae includes signal flow with arbitrary waves, each port normalized to a different and arbitrary reference impedance.
- Identification of a new class of two-port parameters, named *virtual circuit parameters*, to specify arbitrary two-port measurements in a way that is closely related to the equivalent circuit models. This property of being closely related is of significant advantage when specifying measured two-port parameters of bipolar and field effect transistors, without any accuracy limitations of models.

¹ We emphasize that sections 2.1 and most of 2.2 are essentially known microwave concepts. Nevertheless, we observed that many microwave textbooks give an incomplete overview on this subject, and have restricted the validation of the supplied formulae to special cases without further notice. Since these principles are of basic importance for the rest of this book, we start this chapter with a detailed overview of these concepts. We had to consult many textbooks and articles to complete this detailed overview.

2.1. Signal flow observed relative to reference planes

With increasing bandwidth, the dimensions of electronic circuits as well as individual components and their constituent parts become significant with respect to wavelength. In this case, many of the assumptions characteristic of relatively low frequency design lose their validity, and a more fundamental *electromagnetic* signal description increases in relevancy.

This is obvious in the extreme for radio links, antenna design and optics, where the observed dimensions are in the same order of magnitude (or larger) than the wave length of interest. In most practical situations it is however unnecessary to use a full electromagnetic signal description, although we will demonstrate that many of the concepts introduced by microwave engineers are useful to the problem at hand.

In this section 2.1, we review the use of standard microwave methods to define signal flow, matching use of voltage, current and wave methods simultaneously.

single mode transmission

Devices on printed circuit boards (PCB) are interconnected with copper conductors. When individual components are criss-cross interconnected, adequate signal flow is restricted to relatively low frequencies. At higher frequencies, cross-talk effects can be minimized by using copper structures that concentrate the electromagnetic fields in oblong volumes [110], most usually in the form of planar transmission lines above a ground plane.

When designing and characterizing wideband circuits, it is important to restrict signal flow to a single mode². This is because circuit designers prefer simplified descriptions of signal flow using voltages, currents or traveling waves rather than electromagnetic field equations. The signal frequency and the geometry³ of the guiding structure are decisive in determining whether links are single mode or not. For instance, propagation on microstrip lines (see figure 2.1) is quasi-TEM in nature. In practice the TEM approximation is valid to several GHz for 1.5 mm epoxy PCB.

Single mode signal flow facilitates the required simplification because the field in all points of a plane perpendicular to the propagation direction is calculable⁴ when the field is measured in a single point. The consequence is that, one complex number per frequency is adequate for describing forward single-mode transmission. Multi-mode links require additional information for characterizing forward signal flow, and are therefore inconvenient⁵ for transmission purposes.

² In transmission lines, more than one field pattern may fulfill the Maxwell equations as well as the boundary condition of the structure. When no more than one field pattern *propagates* in the transmission line, this link is called a *single mode* link. When more patterns propagate, it is referred as a *multi mode* link.

³ Transmission lines whose diameter is in the same order of magnitude as the wave length of interest, are often single mode transmission lines. In a poorly designed printed circuit board (PCB) with criss-cross links between the devices modes are undefined. The result is that the signal flow may become unpredictable above several MHz. A well-designed PCB with microstrip layout may improve this limit above tens of GHz. These high values usually hold for commonly used coaxial cables (0.5 cm thickness). Rectangular wave guides become multi mode one octave above the cut-off frequency. The first generation fibers (before 1983) were multi mode fibers because the technology was initially unable to handle very small core diameters

⁴ This is restricted to links with unambiguous polarization. This does not hold for structures such as circular wave guides

⁵ A graded-index (multi-mode) fiber with a 50 μ m core typically allows around 500 different core modes, each of which has different signal levels and propagation- and attenuation characteristics. Beyond a certain

We emphasize that a single mode link does not exclude the existence of higher order modes locally. In single mode links, higher order modes damp out quite close to the obstacle that has excited them.

The signal flow in the structure of figure 2.2 is principally single mode at the locations demarcated with solid lines. This is because excited higher order modes do not propagate in this example. The junctions in the center of figure 2.2 may excite higher order modes, which may interact in the vicinity of the dashed line.

signal flow description parameters

A single mode line has two directions of propagation: forward and reverse. Each frequency component of the propagating signal is scaled in magnitude and phase. As a result, two complex numbers per frequency are adequate to provide a full bi-directional description of single mode electromagnetic signal flow.

Voltage and current (U,I) as well as forward and reverse waves (Ψ^+ , Ψ^-) are suitable descriptive pairs for the signal propagation. When the circuit dimension exceeds the wave length of interest, a signal description using waves is commonly preferred. When designing at smaller dimensions or lower frequencies, voltages and currents are more convenient.

Both descriptive methods are identical and are convertible in each other when U and I are well-defined⁶. Both methods are inadequate at locations where higher order modes are excited. Most textbooks focus on one of these two, ignoring or underexposing the other. One aim of this chapter is to discuss them simultaneously in a more balanced way.

length of fiber (up to many kilometers) a steady-state power distribution of fiber modes can be observed to be independent of the launching conditions. Therefore they are applicable under limited conditions.

⁶ Note that the definition of voltage and current in practical links with lossy conductors and isolators is a non-trivial problem.

2.1.1. Signal definition in paired conductor links

When the dimensions of an entire printed circuit board are small, compared to the shortest wavelength of interest, the use of reference planes is of minor importance. In a short conductor the potential is position independent, and all current densities are in phase. As a result, the chosen conductor layout and the reference planes are irrelevant. In wideband circuits however the print layout is as important as the electronic circuit itself. Good design implies the use of well-defined transmission lines.

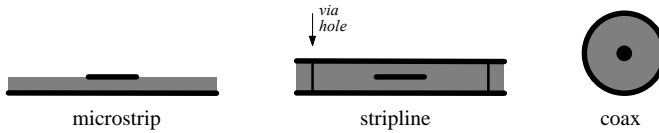


Fig 2.1 Examples of cross-sections of transmission lines. The microstrip and stripline configurations are open configurations and therefore less than ideal. Nevertheless, their fields are mainly concentrated in the dielectric medium between the two conductors which enhances their applicability. The coaxial configuration is completely closed. This prevents electromagnetic interaction with other coaxial transmission lines.

Figure 2.1 shows some examples of well-defined transmission lines, useful to interconnect components and circuits.

- The microstrip is suitable for constructing wideband circuits on printed circuit boards. The bottom side, which is metallized, acts as a ground plane while the copper traces at the top side interconnect all components.
- The stripline is suitable for wideband constructions in multi layer printed circuit board. The two ground planes are interconnected where requested using via holes. A stack of many stripline-layers forms a multi-layer print with minimal mutual coupling between the individual stripline layers.
- The coaxial structure is suitable for interconnection of different circuit blocks.

Figure 2.2 shows some examples of reference planes on a print with a microstrip layout. For a detailed discussion of designing print layout, see van den Brink [110].

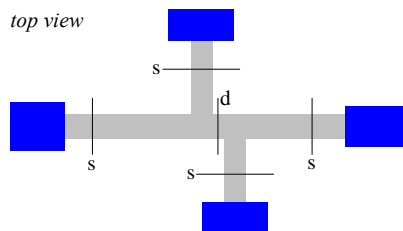


Fig 2.2 Examples of reference planes on a printed circuit board. Four components are interconnected, using a microstrip line. The solid (s) and dashed (d) lines demarcate arbitrary reference planes. At very high frequencies, e.g. above 1 GHz, the signal observed relative to the dotted reference plane may suffer from higher order modes.

Figure 2.3 shows a symbolic representation of the signal flow from a source to a load, observed relative to an arbitrary reference plane. Figure 2.3b defines the single mode waves Ψ from the voltage and the current, assuming that U and I are well-defined⁷. Figure 2.3a shows the reverse transformation.

The reference impedance Z_N is an arbitrary chosen (complex) impedance. Originally, this impedance was chosen to be the (real) characteristic impedance Z_0 of the transmission line, to study scattering effects [204,206]. In 1960, Penfield [207] introduced complex power waves for the discussion of noise performance of negative resistance amplifiers. In 1961 Youla [208] explored the same waves to simplify calculations on power flow. In 1965 Kurokawa [210,211] generalized the theory on waves associated with complex reference impedances.

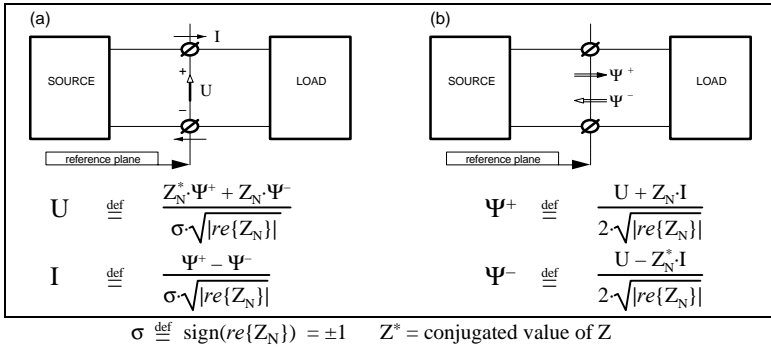


Fig 2.3 The signal flow through reference planes can be described with voltages and currents as well as with waves. The sign correction factor σ extends the validity of the definition to negative reference impedances Z_N .

The definitions, summarized in figure 2.3, are valid for any complex reference impedance, including impedances with negative real part. Many textbook discussions of generalized waves are restricted to complex impedances with positive real part. Some textbooks further restrict the discussion to real reference impedances $R_N = Z_N$. Under these restricted conditions, the signal parameters simplify to:

$$\begin{aligned} U &\rightarrow (\Psi^+ + \Psi^-) \sqrt{R_N} & \Psi^+ &\rightarrow (U + R_N I) / (2 \sqrt{R_N}) \\ I &\rightarrow (\Psi^+ - \Psi^-) / \sqrt{R_N} & \Psi^- &\rightarrow (U - R_N I) / (2 \sqrt{R_N}) \end{aligned}$$

The average power that flows through the reference plane equals $re\{U \cdot I^*\}$. This flow is sometimes referred as transported power, or as transferred power. Using the definitions of figure 2.3 for relating this power flow to waves, it can be easily demonstrated that average power flow is equal to:

$$\langle P \rangle \stackrel{\text{def}}{=} re\{U \cdot I^*\} = \sigma \cdot |\Psi^+|^2 - \sigma \cdot |\Psi^-|^2 = \text{average power flow}$$

⁷ This condition excludes waveguides and fiber-optic links. In these links, the wave concept is more appropriate.

2.1.2. Equivalent load models

For signal flow to a passive linear load, the ratio between the two signal parameters is independent of the signal source. Commonly used ratios are referred to as impedance, admittance or reflection coefficient. Their definition is shown in figure 2.4, when the observation orientation relative to the reference plane is chosen in the direction of the load. The arrows in these equations indicate the simplified definitions when the reference impedance is real $Z_N=R_N$.

load impedance	$Z \stackrel{\text{def}}{=} \frac{U}{I} = \frac{Z_N^* + Z_N \cdot \Gamma}{1 - \Gamma}$	$\rightarrow \frac{1 + \Gamma}{1 - \Gamma} \cdot R_N$
load admittance	$Y \stackrel{\text{def}}{=} \frac{I}{U} = \frac{1 - \Gamma}{Z_N^* + Z_N \cdot \Gamma}$	$\rightarrow \frac{1 - \Gamma}{1 + \Gamma} / R_N$
load reflection coefficient	$\Gamma \stackrel{\text{def}}{=} \frac{\Psi^-}{\Psi^+} = \frac{Z - Z_N^*}{Z + Z_N}$	$\rightarrow \frac{Z - R_N}{Z + R_N}$

Fig 2.4 Definitions of the load model parameters, and how they simplify for real reference impedance $Z_N=R_N$.

The reciprocal value of impedance is admittance. Similarly, a reciprocal definition for reflection coefficient is feasible, although not commonly used. Using the above definitions, the signal parameters are interrelated as follows:

$$\begin{aligned}
 U &= I / Y = \frac{Z_N^* + Z_N \cdot \Gamma}{\sigma \cdot \sqrt{\text{re}\{Z_N\}}} \cdot \Psi^+ = \frac{Z_N^* / \Gamma + Z_N}{\sigma \cdot \sqrt{\text{re}\{Z_N\}}} \cdot \Psi^- && \rightarrow (1 + \Gamma) \cdot \sqrt{R_N} \cdot \Psi^+ \\
 I &= U / Z = \frac{1 - \Gamma}{\sigma \cdot \sqrt{\text{re}\{Z_N\}}} \cdot \Psi^+ = \frac{1 / \Gamma - 1}{\sigma \cdot \sqrt{\text{re}\{Z_N\}}} \cdot \Psi^- && \rightarrow (1 - \Gamma) / \sqrt{R_N} \cdot \Psi^+ \\
 \Psi^+ &= \Psi^- / \Gamma = \frac{1 + Z_N / Z}{2 \cdot \sqrt{\text{re}\{Z_N\}}} \cdot U = \frac{Z + Z_N}{2 \cdot \sqrt{\text{re}\{Z_N\}}} \cdot I \\
 \Psi^- &= \Psi^+ \cdot \Gamma = \frac{1 - Z_N^* / Z}{2 \cdot \sqrt{\text{re}\{Z_N\}}} \cdot U = \frac{Z - Z_N^*}{2 \cdot \sqrt{\text{re}\{Z_N\}}} \cdot I
 \end{aligned}$$

The average power that is consumed (absorbed) in the load equals the average power flow through the reference plane. Its value is for arbitrary values Z_N :

$$\boxed{\langle P_L \rangle \stackrel{\text{def}}{=} |U|^2 \cdot \text{re}\{1/Z\} = |I|^2 \cdot \text{re}\{1/Y\} = \sigma \cdot |\Psi^+|^2 \cdot (1 - |\Gamma|^2)} = \text{consumed power}$$

2.1.3. Equivalent source models

For signal flow from an (active) linear source, the source can be represented by a simple equivalent model. Commonly used equivalent models are Thévenin, Norton and wave models. They are defined in figure 2.5, when the observation orientation relative to the reference plane is chosen in the direction of the load. The associated source parameters are directly extracted from two signal measurements with different (unknown) loads.

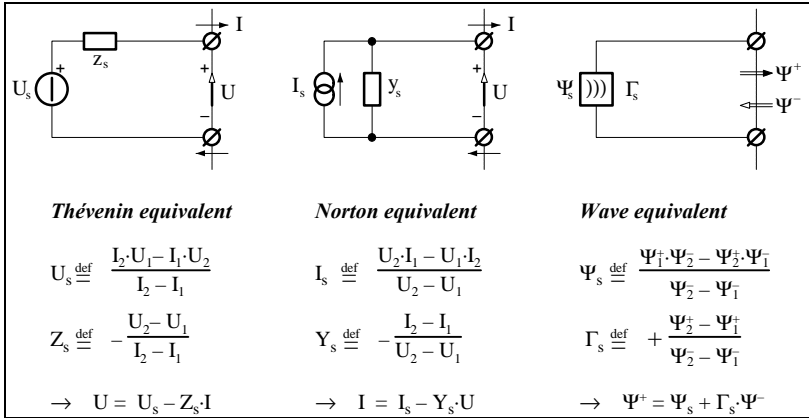


Fig 2.5 Definition of three equivalent models for linear sources, using voltage, currents and waves. The indices "1" and "2" refer to two measurements using different loads.

Many design applications give strong preference to one specific representation of a source. From a *mathematical* point of view, the equivalent models in figure 2.5 are fully transformable to each other. Figure 2.6 and 2.7 show how they are interrelated. Note that the relations between source impedance and reflection coefficient are slightly different from the relations between load impedance and reflection coefficient, shown in figure 2.4. The reference impedances are conjugated because the observation orientation relative to the reference plane is directed towards the load.

<i>Thévenin equivalent</i>	<i>Norton equivalent</i>	<i>Wave equivalent</i>
$U_s = U_s$	$I_s = U_s / Z_s$	$\Psi_s = \frac{\sigma \cdot \sqrt{\text{re}\{Z_N\}}}{Z_s + Z_N^*} \cdot U_s$
$U_s = I_s / Y_s$	$I_s = I_s$	$\Psi_s = \frac{\sigma \cdot \sqrt{\text{re}\{Z_N\}}}{1 + Y_s \cdot Z_N^*} \cdot I_s$
$U_s = \frac{2 \cdot \sqrt{\text{re}\{Z_N\}}}{1 - \Gamma_s} \cdot \Psi_s$	$I_s = \frac{2 \cdot \sqrt{\text{re}\{Z_N\}}}{Z_N + Z_N^* \cdot \Gamma_s} \cdot \Psi_s$	$\Psi_s = \Psi_s$
$Z_s = \frac{Z_N + Z_N^* \cdot \Gamma_s}{1 - \Gamma_s}$	$Y_s = \frac{1 - \Gamma_s}{Z_N + Z_N^* \cdot \Gamma_s}$	$\Gamma_s = \frac{Z_s - Z_N}{Z_s + Z_N}$

Fig 2.6 Relations between the source model parameters. The sign correction factor $\sigma \stackrel{\text{def}}{=} \text{sign}(\text{re}\{Z_N\})$ expands the validity of these models for negative reference impedances.

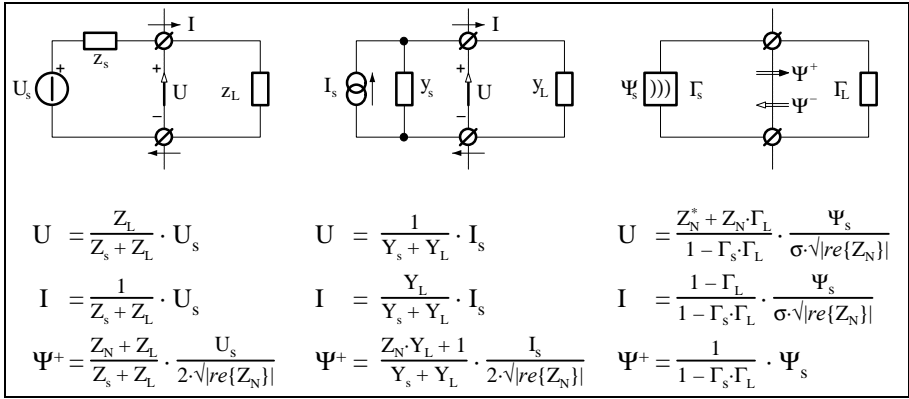


Fig 2.7 Calculation of the signal parameters U , I and Y using the equivalent models for source and load.

The exchangeable source power P_s is the stationary value of the power that will exchange between source and load by arbitrary variation of the load impedance [715,716]. P_s is:

$$\langle P_s \rangle = \frac{|U_s|^2}{4 \cdot \text{re}\{Z_s\}} = \frac{|I_s|^2}{4 \cdot \text{re}\{Y_s\}} = \sigma \cdot (1 - |\Gamma_s|^2) \cdot |\Psi_s|^2 = \text{exchangeable source power}$$

The optimum load conditions for this purpose is when $Z_L = Z_s^*$ or $\Gamma_L = \Gamma_s^*$. When $\text{re}\{Z_s\} > 0$ the maximum available power equals the exchangeable power. When $\text{re}\{Z_s\} < 0$ the maximum available power would always be infinite. Note the very subtle difference in the real parts of Z , Y and Γ between the equations for exchangeable source power and consumed power in the load, since: $\text{re}\{1/Z\} \neq 1/\text{re}\{Z\}$. This is illustrative of the need for care in extending real formulae to complex impedances.

2.1.4. Interconnection transformation of waves

Observation relative to a reference plane has an orientation, which defines the direction of forward (incident) waves (Ψ^+). When the reference impedance is real, then reversal of observation orientation is simply the reversal of forward and reverse waves. This does not hold when the reference impedances are complex.

When observing sources and loads independently, then the chosen observations directions are usually oriented *into* the networks. This makes that both observations will not match when signal flow is analyzed between interconnected networks. It requires an interconnection transformation of observed waves to undo differences in orientation, and if necessary to undo differences in reference impedances.

Figure 2.8 shows two different observations of waves, $\{\Psi_a^+, \Psi_a^-\}$ and $\{\Psi_b^+, \Psi_b^-\}$, of the same signal flow. Reordering of the wave definitions in figure 2.3 results in the following matrix relations:

$$\begin{bmatrix} \Psi_a^+ \\ \Psi_a^- \end{bmatrix} = \frac{1}{2 \cdot \sqrt{\text{re}\{z_a\}}} \begin{bmatrix} 1 & +Z_a \\ 1 & -Z_a^* \end{bmatrix} \cdot \begin{bmatrix} U \\ I \end{bmatrix} \quad \begin{bmatrix} \Psi_b^+ \\ \Psi_b^- \end{bmatrix} = \frac{1}{2 \cdot \sqrt{\text{re}\{z_b\}}} \begin{bmatrix} 1 & +Z_b \\ 1 & -Z_b^* \end{bmatrix} \cdot \begin{bmatrix} U \\ -I \end{bmatrix}$$

$$\begin{bmatrix} U \\ I \end{bmatrix} = \frac{1}{\sigma_a \sqrt{|re\{z_a\}|}} \begin{bmatrix} Z_a^* & Z_a \\ 1 & -1 \end{bmatrix} \cdot \begin{bmatrix} \Psi_a^+ \\ \Psi_a^- \end{bmatrix} \quad \begin{bmatrix} U \\ -I \end{bmatrix} = \frac{1}{\sigma_b \sqrt{|re\{z_b\}|}} \begin{bmatrix} Z_b^* & Z_b \\ 1 & -1 \end{bmatrix} \cdot \begin{bmatrix} \Psi_b^+ \\ \Psi_b^- \end{bmatrix}$$

The transformation of the waves $\{\Psi_a^+, \Psi_a^-\}$ into $\{\Psi_b^+, \Psi_b^-\}$ is simply a matrix product, extracted from the above mentioned relations. The associated *interconnection matrix* Λ is defined in figure 2.8.

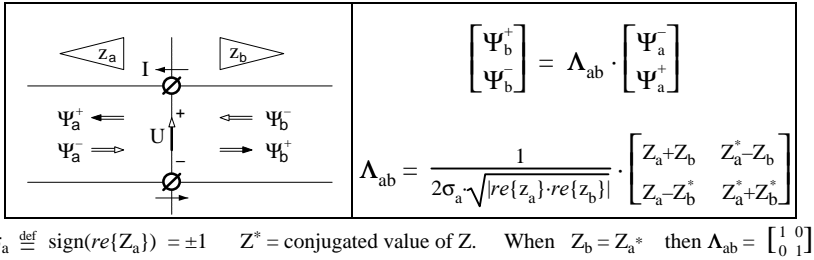


Fig 2.8 Interconnection transformation of waves observed from opposite orientation, each pair normalized to different reference impedances.

When all reference impedances are real and equal then the interconnection transformation is very simple. The interconnection matrix then equals the identity matrix. Transformation is then simplified to exchanging reflected waves with incident waves.

Occasionally, it is convenient to use complex reference impedances [210], for instance to simplify power calculations on waves generated by sources with complex output impedances. Then it is preferred to choose Z_b as the complex conjugate of the reference impedance Z_a . In all other situations the above transformation is required.

2.1.5. Conclusions

Various definitions on signal magnitude, source models and load models are summarized. Our basic philosophy of carrying out observations (measurement) relative to well-defined reference planes, while simultaneously discussing of U , I and Ψ , was introduced. As a result, no specific prior knowledge was required as to sources and loads.

Although no new definitions were introduced, many textbooks and articles have contributed to this overview, since most texts ignore waves and focus on voltages and currents, or are restricted to real impedances, or to complex impedances with positive real part.

The subtle differences between the equations for consumed power and available power demonstrate how risky it is to extend formulae for real impedances to the complex case. The same applies for the subtle differences in the relations between impedance and reflection coefficient in source and load. As will be seen, this overview lays the foundation for the rest of this work.

2.2. Blackbox representation of multi-port networks

Modeling linear⁸ devices as ideal *lumped*⁹ elements is often adequate when designing at relatively low frequencies¹⁰. In these cases, the lumped element values are successfully estimated from low frequency or dc-measurements.

Parasitic capacitive and inductive effects may degrade the validity of low-frequency models. These parasitic effects are considered as *distributed* when the device dimensions cannot be ignored compared to the shortest wavelength (highest frequency) of interest. An infinite number of lumped elements are then required to model these effects, which is considered to be impractical. A well-known example of a distributed effect is delay in transmission lines or transistors.

Wideband circuit analysis requires a mixed analysis of lumped as well as distributed elements. Lumped elements are to be considered as special distributed elements, and each distributed element can be considered as blackbox. These blackboxes are interconnected via ports. When the signal flow through each port is observed relative to well-defined reference planes, the external behavior of each blackbox can be measured at each frequency of interest. These measurements result in blackbox descriptions in tabular form that are directly applicable in microwave circuit simulators.

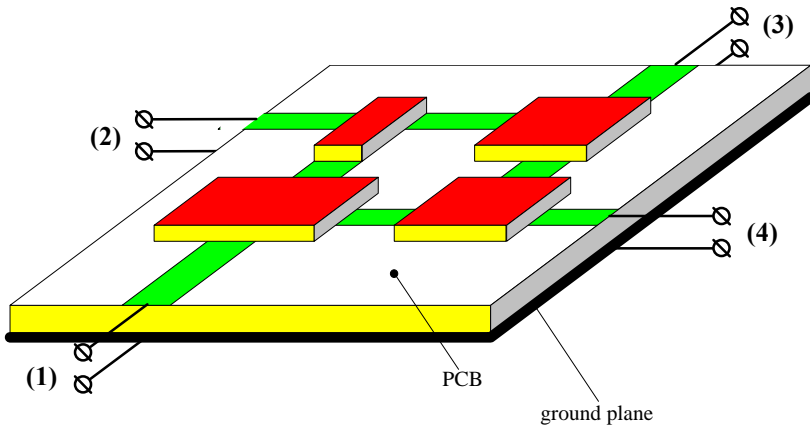


Fig 2.9 An example of a four-port blackbox, which is a sub-circuit that has been cut from a larger PCB (printed circuit board). The component leads are interconnected at the top side of the PCB or grounded using metalized via holes to a uniform copper layer at the bottom side. The edges of this PCB with microstrip layout define the reference planes.

A *linear* blackbox approach, using matrix parameters as description, is applicable over very wide frequency intervals. It remains applicable as long as the signal flow through

⁸ In this text, all *linear* networks are considered as *time invariant* linear networks.

⁹ Lumped elements are ideal elements with zero dimensions and zero delay. Examples are ideal resistors, capacitors, inductors, transformers, and voltage controlled current sources.

¹⁰ The concept 'low frequencies' is highly dependent on the circuit construction. It may be as high as 100 MHz (or higher) when using SMD (surface mounted devices) components on a microstrip print-layout, or as low as 1 MHz (or lower) when all components are at randomly connected to a print with ineffective ground planes.

the reference planes is single mode in nature. This approach in fact restricts the linear analysis to the description of external circuit behavior.

Figure 2.9 shows an example of a four-port blackbox with four well-defined reference planes. It illustrates a piece of a PCB (printed circuit board) that is part of a larger circuit, for instance an amplifier stage of a feedback amplifier with many amplifier stages. The reference planes equal the edges of this piece of PCB.

The thin microstrip construction facilitates that most of the electromagnetic activity is concentrated *in* the (glass-epoxy) dielectric of the PCB. As a result, it is assumed that the radiation is negligible and that the waves pass the reference planes as single mode waves (plane waves).

In section 2.2 we review in short known matrix methods (z-,y-,s-parameters) for the description of multi ports (blackboxes) In addition, we propose virtual circuit methods for describing the transfer of two-port, such as transistors.

2.2.1. Multi-port matrix parameters

Matrix methods are well-known for the use in describing physical multi-port networks. Voltage and current methods (z-, y-parameters) on the one hand and wave methods (s-parameters) on the other have evolved over the last sixty years.

- As early as 1929 [201] Strecker and Feldtkeller proposed these methods, and before 1940 many refinements were added to the theory, for instance [202]. As early as 1953 [205] the application of Z and Y parameters became common place in standard text books on transistor circuit design. Many textbooks have followed since, using matrix methods based on voltages and currents. Many of these texts neglect to mention the existence of S-parameters, associated with a wave description, as an alternative method.
- On the other hand, many classic texts describe wave propagation on transmission lines, using reflection and transmission coefficients. Physicists familiar with wave particle scatter problems, were active at the Radiation Laboratory of M.I.T. in the early 1940's. They applied scattering concepts to the study of wave guide junctions. A summary¹¹ appeared in 1948 by Montgomery [204], and in 1956 Carlin [206] published a detailed analysis on s-parameters¹² with many relevant references. Initially, real reference impedances were used. In 1960, Penfield [207,209] and later Youla [208] introduced s-parameters with complex reference impedances. In 1965, Kurokawa [210,211] generalized the theory, using arbitrary complex reference impedances which are port dependent.

Initially the measurement of multi-port parameters, observed relative to well-defined reference planes, was very laborious. Deschamps [212] proposed in 1953 a graphical method, using slotted lines and movable shorts, to perform full two-port parameter measurements. The introduction in 1967 of automated microwave network analyzers [213,214] simplified these measurements significantly. In the 1970's the popularity of s-parameters increased among engineers due to the growing availability of automated

¹¹ In the years 1942 to 1946 a rather intensive and systematic exploitation of microwave problems was carried out at the Radiation Laboratory of MIT. In the years 1946 to 1952 a group of MIT workers wrote 28 volumes dealing with microwave and related techniques, developed during World-War II.

¹² It was a special issue on scattering parameters, with several other papers on the same subject.

network analyzers. In recent years a growing number of manufacturers have taken to the specification of transistors in terms of s-parameters. Recently, the specification of the s-parameters of passive components (capacitors, inductors) has become more common place.

As a result, methods using z-, y- and s-parameters are now well-known. Nonetheless, no single text was found which reviewed all aspects of the relationship of z-, y-, and s-parameter description in a rigorous way.

<i>definition of symbols</i>	
\mathbf{Z}_N	is diagonal matrix, with arbitrary reference impedances $\{Z_{Nkj}\}$
Z_0	reference impedance when they are all equal and complex
R_0	reference impedance when they are all equal and real
\mathbf{r}_N	is $\sqrt{re\{\mathbf{Z}_N\}}$ is a diagonal matrix with real elements
σ	is $re\{\mathbf{Z}_N\}/re\{\mathbf{Z}_N\}$ is a diagonal matrix with ± 1 elements = $inv(\sigma)$
$\mathbf{1}$	is identity (diagonal) matrix
\mathbf{Z}^*	is the conjugate of matrix \mathbf{Z}
\mathbf{Z}^T	is the normal transpose of matrix \mathbf{Z}
\mathbf{Z}'	is the conjugated transpose of matrix \mathbf{Z} (=adjoint matrix): $\mathbf{Z}' = \mathbf{Z}^{*T}$

Fig 2.10 Definition of symbols that are used in this text. We often prefer Z' as notation for complex conjugated scalars since in that case $Z' = Z^*$.

$\begin{bmatrix} U_1 \\ U_2 \\ \dots \\ U_n \end{bmatrix} = \begin{bmatrix} z_{11} & z_{12} & \dots & z_{1n} \\ z_{21} & z_{22} & \dots & z_{2n} \\ \dots & \dots & \dots & \dots \\ z_{n1} & z_{n2} & \dots & z_{nn} \end{bmatrix} \cdot \begin{bmatrix} I_1 \\ I_2 \\ \dots \\ I_n \end{bmatrix}$	<p>impedance matrix: \mathbf{Z}</p> <p>$\langle P \rangle = \sum_k re\{U_k^* \cdot I_k\}$</p> <p>$\langle P \rangle = re\{\mathbf{U}' \cdot \mathbf{I}\} = re\{\mathbf{U}' \cdot \mathbf{Z} \cdot \mathbf{U}\}$</p>
$\begin{bmatrix} I_1 \\ I_2 \\ \dots \\ I_n \end{bmatrix} = \begin{bmatrix} y_{11} & y_{12} & \dots & y_{1n} \\ y_{21} & y_{22} & \dots & y_{2n} \\ \dots & \dots & \dots & \dots \\ y_{n1} & y_{n2} & \dots & y_{nn} \end{bmatrix} \cdot \begin{bmatrix} U_1 \\ U_2 \\ \dots \\ U_n \end{bmatrix}$	<p>admittance matrix: \mathbf{Y}</p> <p>$\langle P \rangle = \sum_k re\{I_k^* \cdot U_k\}$</p> <p>$\langle P \rangle = re\{\mathbf{I}' \cdot \mathbf{U}\} = re\{\mathbf{I}' \cdot \mathbf{Y} \cdot \mathbf{U}\}$</p>
$\begin{bmatrix} \Psi_{b1} \\ \Psi_{b2} \\ \dots \\ \Psi_{bn} \end{bmatrix} = \begin{bmatrix} s_{11} & s_{12} & \dots & s_{1n} \\ s_{21} & s_{22} & \dots & s_{2n} \\ \dots & \dots & \dots & \dots \\ s_{n1} & s_{n2} & \dots & s_{nn} \end{bmatrix} \cdot \begin{bmatrix} \Psi_{a1} \\ \Psi_{a2} \\ \dots \\ \Psi_{an} \end{bmatrix}$	<p>scattering matrix: \mathbf{S}</p> <p>$\langle P \rangle = \sum_k \sigma_k \cdot \{ \Psi_{ak} ^2 - \Psi_{bk} ^2\}$</p> <p>$\langle P \rangle = \Psi'_a (\sigma \mathbf{S}' \sigma \mathbf{S}) \cdot \Psi_a$</p>
$\Psi_a = (2 \cdot \mathbf{r}_N) \cdot (\mathbf{U} + \mathbf{Z}_N \cdot \mathbf{I})$	$\mathbf{U} = (\sigma \cdot \mathbf{r}_N) \cdot (\mathbf{Z}'_N \cdot \Psi_a + \mathbf{Z}_N \cdot \Psi_b)$
$\Psi_b = (2 \cdot \mathbf{r}_N) \cdot (\mathbf{U} - \mathbf{Z}'_N \cdot \mathbf{I})$	$\mathbf{I} = (\sigma \cdot \mathbf{r}_N) \cdot (\Psi_a + \Psi_b)$

Fig 2.11 Definition of the elementary matrix parameters, and their associated power consumption relations. The symbols are defined in figure 2.10. The orientation of all observations relative to reference planes is directed into the multi-port. It means that the current flow polarity I and the 'approaching' waves Ψ_a are directed into the multi-port. All reference planes may have different reference impedances Z_N to define the waves from the voltages and currents.

In figure 2.10 and 2.11, elementary matrix parameters are defined. They are convenient in combination with modern matrix tools (e.g. Matlab[®] [123]) or modern circuit simulators for handling measured data on multi-port networks.

Z-parameters are convenient in combination with serial impedances and voltage sources). Y-parameters are convenient in combination with shunt admittances and current sources. S-parameters are convenient in combination with waves and scattering problems.

Figure 2.12 shows how these matrix descriptions are related to each other. If desired, the reference impedances Z_N on each port may be chosen differently. This is convenient, for instance, when using transmission lines with 50Ω characteristic impedance and with 75 Ω. It means that Z_N is a diagonal matrix with all (different) reference impedances on its main diagonal.

<i>originating from Z</i>	<i>originating from Y</i>	<i>originating from S</i>
$Z = Z$ $Y = \text{inv}(Z)$ $S = r_N \backslash ((Z - Z_N') / (Z + Z_N)) \cdot r_N$	$Z = \text{inv}(Y)$ $Y = Y$ $S = r_N \backslash ((1 - Z_N' \cdot Y) / (1 + Z_N \cdot Y)) \cdot r_N$	$Z = r_N \cdot ((1 - S) \backslash (S \cdot Z_N + Z_N')) / r_N$ $Y = r_N \cdot ((S \cdot Z_N + Z_N') \backslash (1 - S)) / r_N$ $S = S$
<i>all different real ref. imp.</i> $Z = r_N \cdot ((1 - S) \backslash (S + 1)) \cdot r_N$ $Y = r_N \backslash ((S + 1) \backslash (1 - S)) \cdot r_N$ $S = (r_N \backslash (Z - r_N)) / (r_N \backslash (Z + r_N))$ $S = (1 - r_N \cdot Y \cdot r_N) / (1 + r_N \cdot Y \cdot r_N)$	<i>equal complex ref. imp</i> $Z = (1 - S) \backslash (S \cdot Z_0 + Z_0^* \cdot 1)$ $Y = (S \cdot Z_0 + Z_0^* \cdot 1) \backslash (1 - S)$ $S = (Z - Z_0^* \cdot 1) / (Z + Z_0 \cdot 1)$ $S = (1 - Z_0^* \cdot Y) / (1 + Z_0 \cdot Y)$	<i>equal real ref. imp.</i> $Z = ((1 - S) \backslash (S + 1)) \cdot R_0$ $Y = ((S + 1) \backslash (1 - S)) / R_0$ $S = (Z - R_0 \cdot 1) / (Z + R_0 \cdot 1)$ $S = (1 - R_0 \cdot Y) / (1 + R_0 \cdot Y)$

Fig 2.12 Transformation rules between the matrix parameters of an arbitrary multiport. The validity of these equations includes reference impedances with negative real parts. These rules simplify when all ports use equal reference impedances or when they are real. See figure 2.10 for the definition of the symbols. The matrix division symbols are shortcuts, according to Matlab^a [123] conventions, for:

$$A \backslash B \equiv \text{inv}\{A\} \cdot B \quad A / B \equiv A \cdot \text{inv}\{B\}$$

2.2.2. Multi-port matrix properties

An equivalent matrix description facilitates a full description for arbitrary linear network configurations. This includes active networks with controlled sources, such as voltage controlled current sources. As a result, an arbitrary N-port network requires N² parameters for a full equivalent description.

For a wide range of passive networks, these parameters are interrelated. Well-known physical properties, such as reciprocal and loss-free, result in properties that simplify the matrix. This subsection summarizes these matrix conditions, since they are useful for multi-port analysis.

Reciprocal conditions

Consider an arbitrary network that is completely constructed from reciprocal materials. For a definition of reciprocal media, see [216]. Media for which the conductivity (σ),

permittivity (ϵ) and permeability (μ) are *scalar* quantities at all locations *inside* the network are reciprocal. This does not exclude position-dependency, however, these scalars must be time-invariant and independent of the amplitude and direction of the electric and magnetic field vectors $\underline{\mathbf{E}}$ and $\underline{\mathbf{H}}$.

Let us perform two arbitrary electromagnetic experiments, one that generates the fields $\underline{\mathbf{E}}^{(1)}$ and $\underline{\mathbf{H}}^{(1)}$, and another that generates the field $\underline{\mathbf{E}}^{(2)}$ and $\underline{\mathbf{H}}^{(2)}$. Using the harmonic Maxwell equations¹³ and the Gauss theorem to convert a volume integral to a closed surface integral, it can be demonstrated [211] that the following condition holds:

$$\oiint (\underline{\mathbf{E}}^{(1)} \times \underline{\mathbf{H}}^{(2)} - \underline{\mathbf{E}}^{(2)} \times \underline{\mathbf{H}}^{(1)}) \cdot d\underline{\Omega} \equiv 0$$

When the closed surface of this integral encloses the volume of the multi-port network, this identity provides us a comparative condition for the voltages and currents at all ports. Let's restrict the experiments to a single current source and many voltage probes, one experiment that injects the current in port k and another in port l . Then it can be demonstrated [211] that the reciprocal condition is equivalent with $\{U_k^{(1)} \cdot I_k^{(2)} \equiv U_l^{(2)} \cdot I_l^{(1)}\}$ for any port number k and l . As a result, it can be demonstrated [210,211] that this condition yields the multi-port matrix properties that are summarized in figure 2.13a.

Lossless conditions

In a lossless network the total dissipated power is zero. It means that all power that enters into one port will leave the network via all ports. Integration of the average power flow $re\{\underline{\mathbf{E}} \times \underline{\mathbf{H}}^*\}$ over the closed surface of the network yields for the average power consumption:

$$\oiint re\{\underline{\mathbf{E}} \times \underline{\mathbf{H}}^*\} \cdot d\underline{\Omega} \equiv 0 \quad \text{average power consumption}$$

It can be demonstrated [211] that this condition is equivalent with $re\{\sum_k U_k \cdot I_k^*\} \equiv 0$. This condition yields the multi-port matrix properties that are summarized in figure 2.13b.

(a) <i>reciprocal condition</i> <i>normal transpose</i>	(b) <i>loss-free condition</i> <i>conjugated transpose</i>	(c) <i>reciprocal & loss-free</i> <i>conjugated elements</i>
$\mathbf{Z} \equiv \mathbf{Z}^T \rightarrow z_{kl} \equiv z_{lk}$	$\mathbf{Z} \equiv -\mathbf{Z}'$	$\mathbf{Z} \equiv -\mathbf{Z}^* \equiv j \cdot im\{\mathbf{Z}\}$
$\mathbf{Y} \equiv \mathbf{Y}^T \rightarrow y_{kl} \equiv y_{lk}$	$\mathbf{Y} \equiv \mathbf{Y}'$	$\mathbf{Y} \equiv -\mathbf{Y}^* \equiv j \cdot im\{\mathbf{Y}\}$
$\mathbf{S} \equiv \sigma \cdot \mathbf{S}^T \cdot \sigma \rightarrow s_{kl} \equiv \pm s_{lk}$	$\mathbf{S} \equiv inv(\sigma \cdot \mathbf{S}' \cdot \sigma)$	$\mathbf{S} \equiv inv(\mathbf{S}^*)$

Fig 2.13 Matrix properties for reciprocal, for loss-free and for combined reciprocal loss-free networks. The diagonal matrix \mathbf{S} represents the sign (± 1) of the chosen reference impedance Z_{nk} at each port. (See figure 2.10 for the definition).

Lossless reciprocal conditions

Networks constructed from (quasi) perfect conductors and insulators are (quasi) lossless as well as reciprocal networks. This is because the field strength ($\underline{\mathbf{E}}$, $\underline{\mathbf{H}}$) is zero in perfect conductors and because the conductivity is zero in dielectric media. Similarly to the reciprocal condition it can be demonstrated that this construction is reciprocal as well as

¹³ Maxwell equations: $\nabla \times \underline{\mathbf{H}} = (\sigma + j\omega\epsilon) \cdot \underline{\mathbf{E}}$ and $\nabla \times \underline{\mathbf{E}} = (-j\omega\epsilon) \cdot \underline{\mathbf{H}}$. Gauss: $\iiint (\nabla \cdot \underline{\mathbf{F}}) \cdot dV = \iiint \underline{\mathbf{F}} \cdot d\underline{\Omega}$ and vector identities: $\nabla \cdot (\underline{\mathbf{A}} \times \underline{\mathbf{B}}) = \underline{\mathbf{B}} \cdot (\nabla \times \underline{\mathbf{A}}) - \underline{\mathbf{A}} \cdot (\nabla \times \underline{\mathbf{B}})$

loss-free. As a result, it can be demonstrated [211] that the combination of the matrix identities in figure 2.13a and 2.13b yields the additional relations of figure 2.13c. Other properties, such as symmetry or asymmetry between two ports will result in additional matrix identities, which are beyond the scope of this short overview.

2.2.3. Multi-port matrix reduction algorithm

Consider a circuit with N_n nodes, represented by an $N_n \times N_n$ matrix (z-, y- or s-parameters). In many circuit applications, no more than a few nodes ($N_p < N_n$) are externally available, for instance nodes p_1 and p_2 (the port nodes). This means that the current vector \mathbf{I} has many zero coefficients except at row p_1 and p_2 . Furthermore, it means that most coefficients of the voltage vector \mathbf{U} are not of interest, except at row p_1 and p_2 . This ascertainment provides the means to reduce the matrix dimension from $N_n \times N_n$ down to $N_p \times N_p$.

When the matrix representation is transformed into z-parameters ($\mathbf{U}=\mathbf{Z}\cdot\mathbf{I}$) most coefficients of \mathbf{Z} are multiplied with the zero coefficients in the current vector \mathbf{I} . Furthermore, most calculated coefficients in the voltage vector \mathbf{U} are not of interest. As a result, most coefficients in \mathbf{Z} are unused and the reduced impedance matrix \mathbf{z} results from \mathbf{Z} by deleting all rows and columns except those with number p_1 and p_2 .

This procedure of row and column deletion is simply described using an auxiliary matrix \mathbf{P} (port definition matrix) of the following general form:

$$\mathbf{P} \stackrel{\text{def}}{=} \begin{bmatrix} 1 & 0 \\ 0 & 0 \\ 0 & 1 \\ 0 & 0 \\ 0 & 0 \\ 0 & 0 \\ 0 & 0 \end{bmatrix} \begin{array}{l} \leftarrow \text{row } p1 \\ - \\ \leftarrow \text{row } p2 \\ - \\ - \\ - \\ - \end{array} \quad \Rightarrow \quad \boxed{\mathbf{z} = \mathbf{P}' \cdot \mathbf{Z} \cdot \mathbf{P}} \quad \text{and} \quad \mathbf{P}' \cdot \mathbf{P} = \mathbf{1}$$

This simple matrix identity is reserved for z-parameters only. Reduction of y- and s-parameters requires z-parameters as intermediate representation format. Use the transformation rules of figure 2.12 for this purpose, for instance: $\mathbf{y} = \text{inv}(\mathbf{P}' \cdot \mathbf{Y} \cdot \mathbf{P})$.

Reducing y- and s-parameters by deleting rows and columns, is equivalent with connecting the reduced nodes to ground via an impedance $Z=0$ or $Z=Z_N$ respectively.

This reduction algorithm is important for extracting various feedback parameters from arbitrary circuits in which the feedback network is specified as four-port and the forward amplifier as two-port (see section 4.2). The multi-port parameters of these sub-circuits are derived from arbitrary circuits using a circuit simulator, for instance the simulator described in section 2.2.4 and 7.2.4.

Moreover, this algorithm is important for deriving fundamental network properties, such as the generalized thermal noise theorem described in section 7.2.5.

2.2.4. Application of multi-port transfer matrices in circuit simulators

A very simple circuit simulator can be realized when using y-parameters because admittance matrix parameters are convenient when shunting circuits. A complex circuit is simply the shunted combination of many sub-circuits, each of them described with y-parameters. The *nodal admittance matrix method* described here can be found in various textbooks dealing with computer aided circuit analysis, for instance Dobrowolski [724].

Because our integrated approach of designing and characterizing wideband circuits relies extensively on various computer algorithms, this section discusses algorithms for automated circuit analysis. It facilitates the exploration of new feedback analysis and synthesis concepts, as introduced in chapter 4 and 5.

Consider two circuits, represented by \mathbf{Y}_1 and \mathbf{Y}_2 . When the node voltages of these circuits equal the voltages \mathbf{U}_1 and \mathbf{U}_2 , the associated currents equal $\mathbf{I}_1=\mathbf{Y}_1\cdot\mathbf{U}_1$ and $\mathbf{I}_2=\mathbf{Y}_2\cdot\mathbf{U}_2$. In the special case that all nodes are interconnected then $\mathbf{U}_1=\mathbf{U}_2$. This is associated with a combined current flow of $(\mathbf{I}_1+\mathbf{I}_2)=(\mathbf{Y}_1+\mathbf{Y}_2)\cdot\mathbf{U}$. As a result, the admittance matrix of the combined circuit is simply the sum of the individual \mathbf{Y} -matrices.

A simple circuit simulator [116,118] uses this property to construct the admittance matrix of complex circuits. All node numbers of the circuit are associated with a corresponding (unique) row and column number of this matrix. The ground node is zero, and corresponds with a (dummy) row and column number zero. This row and column, will be deleted afterwards. The simulator starts from an empty circuit ($\mathbf{Y}=\mathbf{0}$), and a distinct frequency of interest. Each circuit element (impedance, VCCS, etc.) is subsequently added to \mathbf{Y} by calculating its individual y -parameters. This procedure is summarized below:

- An impedance Z , connected from node n_1 to n_2 , is represented by a 2×2 admittance matrix. Its four coefficients are added to four coefficients of the main \mathbf{Y} matrix, that corresponds with the specified node numbers. This addition equals with:

$$\begin{bmatrix} y_{n1,n1} & y_{n1,n2} \\ y_{n2,n1} & y_{n2,n2} \end{bmatrix} = \begin{bmatrix} y_{n1,n1} & y_{n1,n2} \\ y_{n2,n1} & y_{n2,n2} \end{bmatrix} + 1/Z \cdot \begin{bmatrix} 1 & -1 \\ -1 & 1 \end{bmatrix} \quad n1 \bullet \text{---} \boxed{Z} \text{---} \bullet n2$$

- A VCCS (voltage controlled current source) is essentially a four-port and must be represented by a 4×4 admittance matrix. Since it is a floating circuit, most coefficients are zero. No more than four non-zero coefficients are left, and they are added to the associated coefficients in the main \mathbf{Y} matrix. This addition is:

$$\begin{bmatrix} y_{n2,n1} & y_{n2,n3} \\ y_{n4,n1} & y_{n4,n3} \end{bmatrix} = \begin{bmatrix} y_{n2,n1} & y_{n2,n3} \\ y_{n4,n1} & y_{n4,n3} \end{bmatrix} + g \cdot \begin{bmatrix} 1 & -1 \\ -1 & 1 \end{bmatrix} \quad n1 \bullet \text{---} \begin{array}{c} + \\ \text{g} \\ - \end{array} \text{---} \bullet n2 \\ n3 \bullet \text{---} \begin{array}{c} - \\ \text{g} \\ + \end{array} \text{---} \bullet n4$$

- A transmission line is most conveniently modeled in s -parameters. These s -parameters are converted into y -parameters, and then added to \mathbf{Y} .
- Most other circuit elements, such as transistor models and opamps are modeled with a combination of impedances and VCCS elements.

When all elements of the net-list are inserted, the combined admittance matrix \mathbf{Y} of the circuit is complete. The inverse matrix provides the impedance matrix \mathbf{Z} of the circuit. The circuit simulator must now reduce this matrix to a smaller matrix, for instance a 2×2 matrix \mathbf{z} of a two-port.

As described in section 2.2.3, the reduces impedance matrix equals:

$$\boxed{\mathbf{z} = \mathbf{P}' \cdot \mathbf{Z} \cdot \mathbf{P} = \mathbf{P}' \cdot (\mathbf{Y} \setminus \mathbf{P})}$$

The circuit simulator has completed when all \mathbf{z} matrices are evaluated for all frequencies of interest. When s - or y -parameters are preferred, convert all \mathbf{z} matrices into the preferred format. The dimension of matrix \mathbf{z} depends on the number of ports of the circuit.

We realized the above simulator in the 4GL computer language MatLab® [123], and found that less than four pages source code are adequate for implementing this simulator

2.2.5. Conclusions

Standard matrix methods for the representation of linear networks have been summarized. The overview has focused on a simultaneous discussion of z-, y- and s-parameters, without any restrictions on port reference impedance (Z_N).

Although these methods are well-known, most textbook discussions are restricted to real reference impedances, to positive complex reference impedances or to reference impedances that are equal at all ports.

Matrix expressions have been discussed for transforming N-port parameters into M-port parameters ($M < N$). The matrix notation of these expressions is convenient for proving various properties of arbitrary networks and for evaluating transfer functions in circuit simulators.

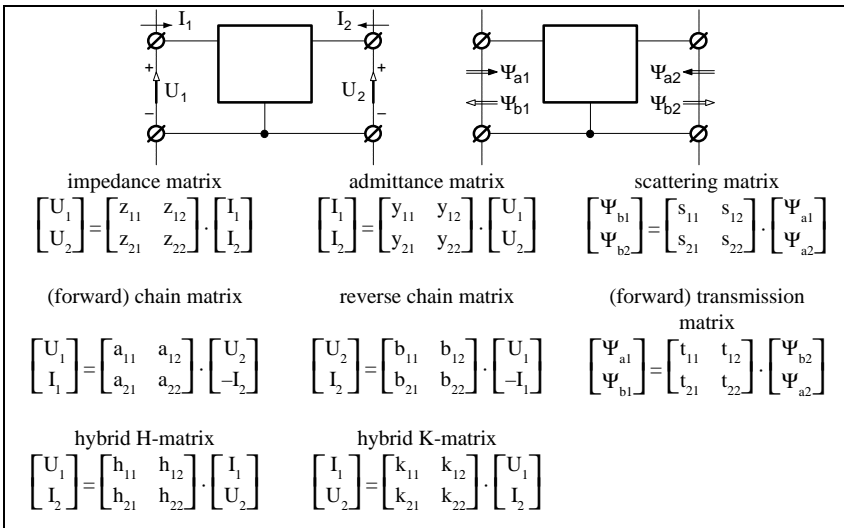
2.3. Two-port transfer parameters

An important group of multi-port parameters are two-port parameters. One of the reasons is that they are directly available from measurements with commercially available network analyzers. As a result, an increasing number of manufacturers is specifying their components (transistors, inductors, etc.) in two-port parameters, usually in s-parameter format.

This section discusses the well-known two-port matrix parameters and introduces a new class of parameters: *virtual circuit parameters*.

2.3.1. Two-port matrix parameters

In addition to previously defined z-, y- and s-parameters, many other formats are in use. This is because reorganization of the matrix equations may simplify the calculation of cascaded two-ports, or may simplify other specialized calculations. Unfortunately, different names and letters are in use for identical parameter formats. Figure 2.14 shows an overview of some preferred¹⁴ matrix parameter formats.



$$\begin{bmatrix} a_{11} & a_{12} \\ a_{21} & a_{22} \end{bmatrix} = \begin{bmatrix} A & B \\ C & D \end{bmatrix} = \begin{bmatrix} 1/\mu & 1/\gamma \\ 1/\zeta & 1/\alpha \end{bmatrix} = \begin{bmatrix} 1/T_{uu} & 1/T_{iu} \\ 1/T_{ui} & 1/T_{ii} \end{bmatrix}$$

$$\begin{bmatrix} k_{11} & k_{12} \\ k_{21} & k_{22} \end{bmatrix} = \begin{bmatrix} g_{11} & g_{12} \\ g_{21} & g_{22} \end{bmatrix}$$

Fig 2.14 Matrix definitions for two-port networks. The definitions inside the borderline are recommended by IEC standards [215] or commonly used in microwave literature. The other matrices are equivalent definitions that are also often used.

¹⁴ The matrix symbols Z, Y, A, B, H and K are recommended by IEC standards [215] (no 3-506 to 3-511). The s- and t-parameters are not mentioned in this standard, nor the commonly used [A,B,C,D] parameters.

Analyzing a cascade of two-ports is simple when chain parameters (**A**) or transmission parameters (**T**) are used. The two-port parameters of the cascade then result from a simple matrix product of the individual two-ports matrices. These products are:

$$\begin{aligned} \text{voltage and currents:} \quad & \mathbf{A} = \mathbf{A}_1 \cdot \mathbf{A}_2 \cdot \mathbf{A}_3 \cdot \dots \mathbf{A}_n \\ \text{waves:} \quad & \mathbf{T} = \mathbf{T}_1 \cdot \mathbf{\Lambda}_{12} \cdot \mathbf{T}_2 \cdot \mathbf{\Lambda}_{23} \cdot \mathbf{T}_3 \cdot \mathbf{\Lambda}_{34} \cdot \dots \mathbf{T}_n \end{aligned}$$

The matrices **A** represent the interconnection transformation matrix of waves, when reference plane orientation and reference impedance do not match. This is discussed in detail in section 2.1.4. When they do match, for instance because all reference impedances are real and equal, then an interconnection transformation is superfluous because $\mathbf{\Lambda} \equiv \mathbf{I}$.

With the exclusion of a very limited number of exceptional cases, two-port matrix parameter descriptions are mutually transformable. When the reference impedances are positive real, then these relations simplify significantly. Figure 2.15 summarizes some of these relations in matrix format. Appendix A summarizes similar relations between the elements of the matrices.

$\mathbf{Z} = (\mathbf{Y}\mathbf{I})$ $\mathbf{Z} = (\mathbf{A}\cdot\mathbf{I}_3 - \mathbf{I}_1) \setminus (\mathbf{I}_2 + \mathbf{A}\cdot\mathbf{I}_4)$ $\mathbf{Z} = (\mathbf{H}\cdot\mathbf{I}_4 - \mathbf{I}_1) \setminus (\mathbf{I}_4 - \mathbf{H}\cdot\mathbf{I}_1)$ $\mathbf{Z} = \mathbf{r}_N \setminus ((\mathbf{I} - \mathbf{S}) \setminus (\mathbf{I} + \mathbf{S})) \cdot \mathbf{r}_N$	$\mathbf{Y} = (\mathbf{Z}\mathbf{I})$ $\mathbf{Y} = (\mathbf{I}_2 + \mathbf{A}\cdot\mathbf{I}_4) \setminus (\mathbf{A}\cdot\mathbf{I}_3 - \mathbf{I}_1)$ $\mathbf{Y} = (\mathbf{I}_4 - \mathbf{H}\cdot\mathbf{I}_1) \setminus (\mathbf{H}\cdot\mathbf{I}_4 - \mathbf{I}_1)$ $\mathbf{Y} = \mathbf{r}_N \setminus ((\mathbf{I} + \mathbf{S}) \setminus (\mathbf{I} - \mathbf{S})) \cdot \mathbf{r}_N$	$\mathbf{S} = (\mathbf{r}_N \setminus \mathbf{Z} - \mathbf{r}_N) / (\mathbf{r}_N \setminus \mathbf{Z} + \mathbf{r}_N)$ $\mathbf{S} = (\mathbf{I} - \mathbf{r}_N \cdot \mathbf{Y} \cdot \mathbf{r}_N) / (\mathbf{I} + \mathbf{r}_N \cdot \mathbf{Y} \cdot \mathbf{r}_N)$ $\mathbf{S} = (\mathbf{T} \cdot \mathbf{I}_3 - \mathbf{I}_2) \setminus (\mathbf{I}_1 - \mathbf{T} \cdot \mathbf{I}_4)$
$\mathbf{A} = (\mathbf{I}_1 \cdot \mathbf{Z} + \mathbf{I}_2) / (\mathbf{I}_3 \cdot \mathbf{Z} - \mathbf{I}_4)$ $\mathbf{A} = (\mathbf{I}_1 + \mathbf{I}_2 \cdot \mathbf{Y}) / (\mathbf{I}_3 - \mathbf{I}_4 \cdot \mathbf{Y})$ $\mathbf{A} = (\mathbf{I}_1 \cdot \mathbf{H} + \mathbf{I}_2) / (\mathbf{I}_3 - \mathbf{I}_4 \cdot \mathbf{H})$	$\mathbf{H} = (\mathbf{I}_1 \cdot \mathbf{Z} + \mathbf{I}_4) / (\mathbf{I}_1 + \mathbf{I}_4 \cdot \mathbf{Z})$ $\mathbf{H} = (\mathbf{I}_1 + \mathbf{I}_4 \cdot \mathbf{Y}) / (\mathbf{I}_1 \cdot \mathbf{Y} + \mathbf{I}_4)$ $\mathbf{H} = (\mathbf{A} \cdot \mathbf{I}_4 + \mathbf{I}_1) \setminus (\mathbf{A} \cdot \mathbf{I}_3 - \mathbf{I}_2)$	$\mathbf{T} = (\mathbf{I}_1 + \mathbf{I}_2 \cdot \mathbf{S}) / (\mathbf{I}_3 \cdot \mathbf{S} + \mathbf{I}_4)$

$$\mathbf{I} = \begin{bmatrix} 1 & 0 \\ 0 & 1 \end{bmatrix} \quad \mathbf{I}_1 = \begin{bmatrix} 1 & 0 \\ 0 & 0 \end{bmatrix} \quad \mathbf{I}_2 = \begin{bmatrix} 0 & 0 \\ 1 & 0 \end{bmatrix} \quad \mathbf{I}_3 = \begin{bmatrix} 0 & 1 \\ 0 & 0 \end{bmatrix} \quad \mathbf{I}_4 = \begin{bmatrix} 0 & 0 \\ 0 & 1 \end{bmatrix} \quad \mathbf{r}_N = \begin{bmatrix} \sqrt{Z_{N1}} & 0 \\ 0 & \sqrt{Z_{N2}} \end{bmatrix}$$

Fig 2.15 Some transformation rules between various two-port matrices when the two (different) reference impedances are positive real.

Arbitrary multi-port networks that include one or more sources are described in section 7.2 when discussing noise. The review in this chapter is restricted to networks in which a single embedded source is connected to an output port via two-port networks. These configurations are shown in figure 2.16.

When these two-port parameters are known then the internal characteristics of this source are calculable from the external values, and visa-versa. This procedure is equivalent to repositioning a reference plane from an external accessible position to an internal position, or reversal. Figure 2.16 summarizes an overview of transformation rules for embedding and de-embedding of sources.

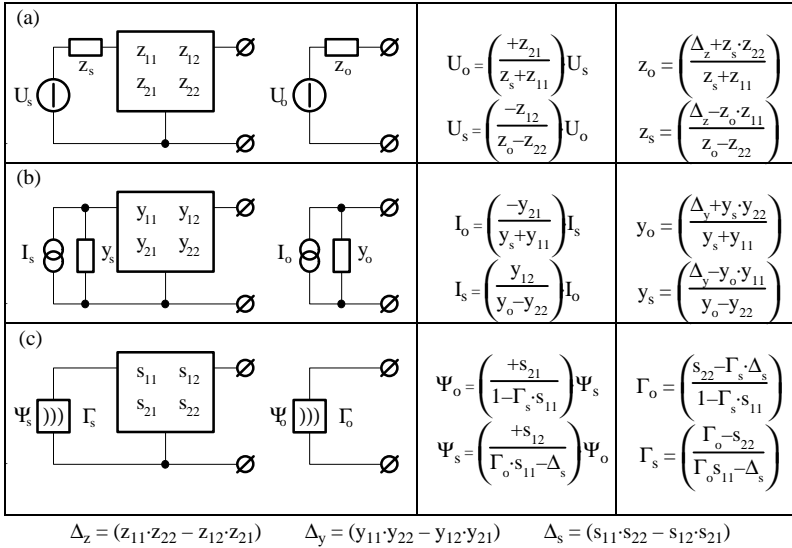


Fig 2.16 Embedding and de-embedding relations for sources.

2.3.2. Two-port virtual circuit parameters

Matrix parameters are convenient for performing two-port network calculations with computers and for representing transfer measurements. Four (measured) parameters per frequency are adequate to represent a linear two-port in tabular form. For instance, an analysis for 50 frequencies requires a table with 200 complex numbers.

Some matrix representations are more convenient for a specific job, Z-parameters are convenient when networks are connected in series, y-parameters when networks are in shunt, and s-parameters when signals are transported through transmission lines. This has caused that network analyzers usually measure s-parameters.

This is not the only matrix way for representing data from two-port measurements. With the exclusion of numerical round-off errors and a very limited number of exceptional cases, it does not really matter whether the two-port measurements are presented in s-, t-, h-, z-, a- or y-format, because all these two-port representations are mutually transformable.

Another well-known approach of describing two-ports are equivalent circuit models. These circuits are constructed with a finite number of ideal lumped elements to model the two-port. This approach facilitates an *approximate* description, and has in essence a physical meaning. The meaning of matrix parameters is in essence abstract, which facilitates an *exact* description for arbitrary linear two-ports.

We propose the identification of an additional class of two-port parameters: *virtual*¹⁵ *circuit parameters*. Similarly to other matrix parameter sets they are nonphysical in

¹⁵ We chose the name *virtual* circuits to designate it from *equivalent* circuits. Equivalent circuits usually originates on physical grounds while the meaning of virtual circuits is in essence abstract.

nature although their meaning is closely related to a simple behavioral model. For instance, amplifier blocks are often represented by an input impedance, an output impedance, a controlled source to represent gain and a controlled source to represent isolation. It means that it is characterized with a virtual circuit in stead of an equivalent circuit model. In general, virtual circuits have no physical relation to the actual amplifier. Virtual circuit parameters represent the elements of a pre-defined virtual circuit

An important aspect of virtual circuit parameters is that they are reversibly transformable from standard matrix descriptions. To enable a reverse transform two-port virtual circuits consist of exactly four independent elements. This restriction is essential for virtual circuits, while equivalent circuit models may contain any number of elements.

The advantage of two-port virtual circuit parameters is that they provide an exact description of two-ports while they have been found more appropriate for manual interpretation of two-port data than matrix parameters

Two-port virtual circuit parameters are a set of four complex numbers per frequency. Electronic circuit models, constructed with exactly four *independent* elements, are suitable for this purpose. There are many possible circuit topologies that may represent an arbitrary two-port with four independent (virtual) elements. Figure 2.17 shows some examples, using a single controlled current source and three impedances.

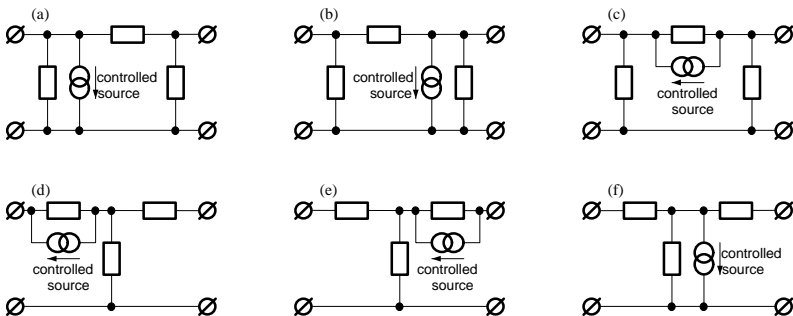


Fig 2.17 Some virtual circuit topologies that facilitate a full representation of an arbitrary linear two-port. The controlled sources are controlled by a voltage over an impedance or by a current through an impedance.

When the four-element topology is chosen, then the virtual circuit parameters can be found simply from a given matrix description. Y-parameters are often convenient for Π -topologies and z-parameters are often convenient for T-topologies. There is a reversible parameter transformation, for each frequency of interest. When the two-port is reciprocal, three virtual elements are adequate, since the matrix parameters are interrelated (see figure 2.13).

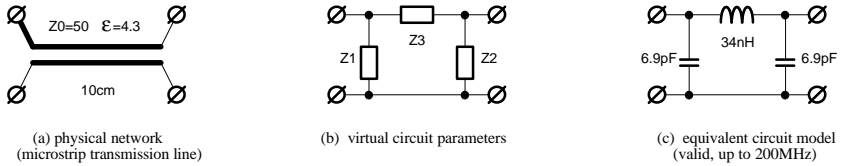


Fig 2.18 An application example of virtual circuit parameters. They simplify the validity assessment of lumped approximations of distributed networks. It can be demonstrated that the following conditions hold:
 $z_1=1/(y_{11}-y_{12})$, $z_2=1/(y_{22}+y_{12})$, $z_3=1/(-y_{12})$.

The use of virtual circuit parameters often facilitates the assessment of a lumped approximation to a distributed network. Figure 2.18a shows a well-known example of a distributed network, namely a microstrip transmission line on a standard epoxy print. The s -parameters are calculated or measured, and subsequently transformed to y -parameters to simplify the evaluation of the virtual circuit parameters.

Figure 2.18b shows the chosen virtual circuit topology. Since the two-port is reciprocal, three virtual circuit parameters are adequate. All virtual impedances Z_1 , Z_2 and Z_3 are frequency dependent.

Bode plots of Z_1 and Z_3 indicate that this frequency dependence is proportional to $(1/j\omega)$ and $(j\omega)$ respectively, over a wide frequency interval. This is confirmed by plotting $1/(j\omega \cdot Z_1)$ and $(Z_3/j\omega)$, as is shown in figure 2.19. It illustrates that Z_1 is capacitive up to 400 MHz and that Z_3 is inductive up to 200 MHz. As a result, the equivalent circuit in figure 2.18c is an adequate lumped element approximation up to 200 MHz.

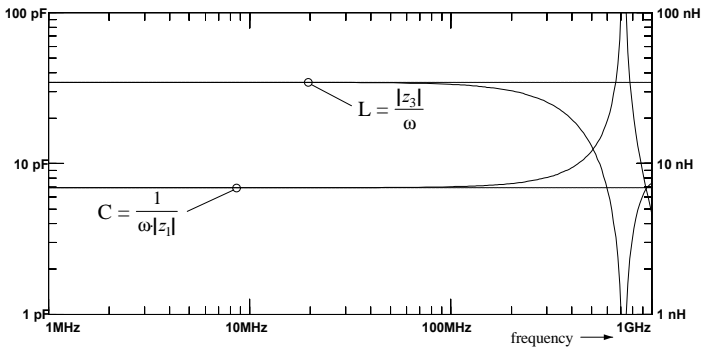


Fig 2.19 Bode plots of $1/(j\omega \cdot Z_1)$ and $(Z_3/j\omega)$, associated with the virtual circuit parameters Z_1 and Z_3 of the two-port in figure 2.18. The curves are flat over a wide frequency interval, indicating that Z_1 is capacitive up to 400 MHz and Z_3 is inductive up to 200 MHz.

Virtual circuit parameters provide an attractive graphical specification method for transistors. For discrete transistors, they can be extracted from s -parameter measurements at bias conditions of interest. For integrated transistors they must be extracted from sophisticated (non linear) device models that have various process-dependent parameters as input. More and more transistor manufacturers are also

specifying their discrete transistors in two-port parameters, usually s-parameters (tabular and graphical). These presentation formats are convenient for use with software tools and in 50Ω transmission line applications, although they are often inconvenient in other applications.

We have found plots of representative data, presented in a form that is closely related to a simple transistor model, to be preferable. This is quite different from specifying the parameters of a model, since models are approximations and virtual circuit parameters not. Finding the most convenient virtual circuit topology is a matter of trial and error in practice. A good choice is a topology in which the four virtual elements can be approximated by ideal lumped elements over the frequency interval of interest.

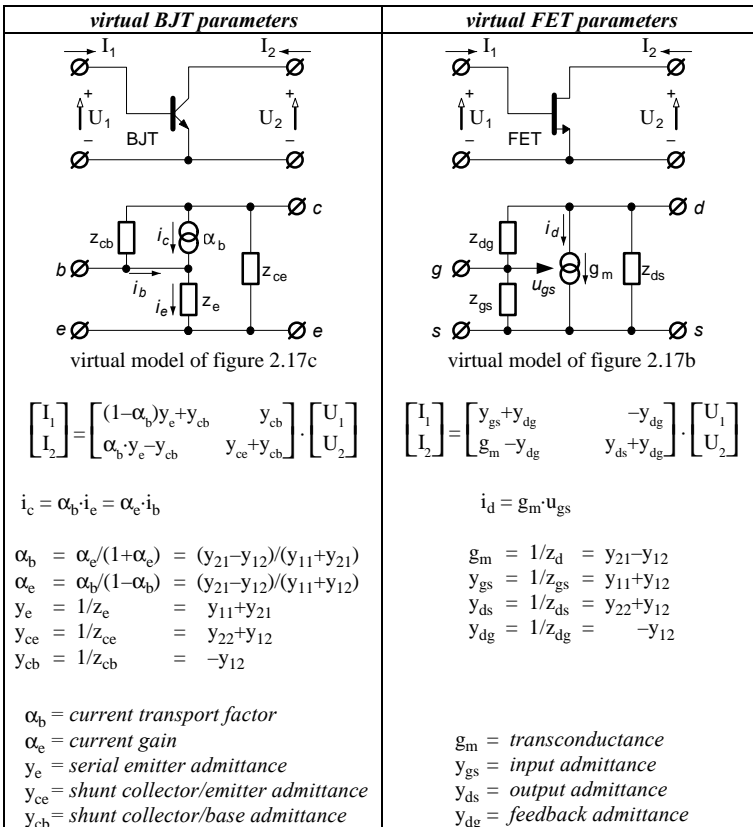


Fig 2.20 Definition of two-port virtual circuit parameters for transistors. These parameters are $[\alpha_e, z_e, z_{ce}, z_{cb}]$ or $[\alpha_b, z_e, z_{ce}, z_{cb}]$ for a BJT, and $[g_m, z_{gs}, z_{ds}, z_{dg}]$ for an FET.

Figure 2.20 shows convenient topologies for BJT's (bipolar junction transistors) and FETs (field effect transistors). They provide the virtual parameter sets $[\alpha_e, z_e, z_{ce}, z_{cb}]$ or $[\alpha_b, z_e, z_{ce}, z_{cb}]$ for a BJT, and $[g_m, z_{gs}, z_{ds}, z_{dg}]$ for an FET. These virtual values are

unique for a specific topology, and they are reversibly transformable from standard two-port matrix parameters¹⁶.

The plots in section 3.2.1, show virtual parameter plots of *measured* transistor data. These plots represent the behavior models of figure 2.17b and c. The fact that their values match very well with ideal elements demonstrates how attractive this novel descriptive method can be.

2.3.3. Conclusions

Standard matrix methods for the representation of linear two-ports have been summarized, being an important group of multi-port matrix parameters.

We propose in a natural way the identification of a new class of network parameters: *virtual circuit parameters*. They are convenient for assessing the validity of simple lumped element approximations to distributed networks. In addition, a convenient set of virtual circuit parameters for BJT's (bipolar junction transistors) and FETs (field effect transistors) has been selected. A set of virtual parameter plots of measured transistor data combines the advantages of an exact *linear* specification with those of simple though adequate transistor models.

This section provided the mathematical tools for transforming measured two-port data into a form that is most convenient for the given application.

¹⁶ Keep in mind that the transistor is assumed to be biased linearly!